ISSN (print): 1698-6180. ISSN (online): 1886-7995
www.ucm.es/info/estratig/journal.htm

Journal of Iberian Geology 33 (2) 2007: 191-206

Journal of Iberian Geology
AN INTERNATIONAL PUBLICATION OF EARTH SCIENCES

Sandstone petrofacies in the northwestern sector of the Iberian Basin

Petrofacies arenosas en el sector noroccidental de la Cuenca Ibérica

J. Arribas[1], M. Ochoa[1], R. Mas[2], Mª E. Arribas[1], L. González-Acebrón[2]

[1]Dpto. de Petrología y Geoquímica, Univ. Complutense de Madrid – CSIC, c/ Jose Antonio Novais 2, 28040 Madrid, Spain (arribas@geo.ucm.es; mochoa@geo.ucm.es; earribas@geo.ucm.es)
[2]Dpto. de Estratigrafía, Univ. Complutense de Madrid – CSIC, c/ Jose Antonio Novais 2, 28040 Madrid, Spain (ramonmas@geo.ucm.es; lgcebron@geo.ucm.es)

Received: 10/05/06 / Accepted: 06/07/06

Abstract

During the most active rifting stages in the northwestern sector of the Iberian Basin (Cameros Basin and Aragonese Branch of the Iberian Range), thick sequences of continental clastic deposits were generated. Sandstone records from Rift cycle 1 (Permo-Triassic) and Rift cycle 2 (Late Jurassic-Early Cretaceous) show similarities in composition. Based on the most recent data, this paper describes sandstone petrofacies developed during both rifting periods. Six petrofacies can be distinguished: two associated with Rift cycle 1 (PT-1 and PT-2) and four with Rift cycle 2 (JC-1 to JC-4). All six petrofacies can be classified as sedimentoclastic or plutoniclastic.

Sedimentoclastic petrofacies developed during early rifting stages either through the recycling of pre-rift sediments or significant palaeogeographical changes. These facies comprise a thin succession (<100 m) of clastic deposits with mature quartzose and quartzolithic sandstones containing sedimentary and metasedimentary rock fragments. Carbonate diagenesis is more common than clay mineral diagenesis. Sedimentoclastic petrofacies have been identified in Rift cycle 1 (Saxonian facies, PT-1) and Rift cycle 2 (JC-1 and JC-3; Tithonian and Valanginian, respectively). In the absence of the pre-rift sedimentary cover, metasedimentoclastic petrofacies sometimes develop as a product of the erosion of the low- to medium-grade metamorphic substratum (Petrofacies JC-2, Tithonian-Berriasian).

Plutoniclastic petrofacies were generated during periods of high tectonic activity and accompanied by substantial denudation and the erosion of plutonites. Forming thick stratigraphic successions (1000 to 4000 m), these feldspar-rich petrofacies show a rigid framework and clay mineral diagenesis. In Rift cycle 1, plutoniclastic petrofacies (PT-2) are associated with the Buntsandstein. This type of petrofacies also developed in Rift cycle 2 in the Cameros Basin (JC-4) from DS-5 to DS-8 (Hauterivian-Early Albian), and represents the main basin fill interval.

Sedimentoclastic and plutoniclastic petrofacies can be grouped into three pairs of basic petrofacies. Each pair represents a 'provenance cycle' that records a complete clastic cycle within a rifting period. Petrofacies PT-1 and PT-2 represent the 'provenance cycle' during Rift-1. In the Cameros Basin, two provenance cycles may be discerned during Rift cycle 2, related both to the Tithonian-Berriasian and the Valanginian-Early Albian megasequences.

Tectonics is the main factor controlling petrofacies. Other factors (e.g., maturation during transport, local supply) may modulate

the compositional signatures of the petrofacies yet their main character persists and even outlines the hierarchy of the main bounding surfaces between depositional sequences in the intracontinental Iberian Rift Basin.

Keywords: Sandstone provenance, petrofacies, Rift Basins, Iberian Range, Permo-Triassic, Early Cretaceous.

Resumen

Durante las fases de rifting más activas en el sector noroccidental de la Cuenca Ibérica (Cuenca de Cameros y Rama Aragonesa de la Cordillera Ibérica), se generaron potentes sucesiones detríticas de depósitos continentales. Los registros arenosos del ciclo Rift 1 (Permo-Triásico) y Rift-2 (Jurásico Superior-Cretácico Inferior) muestran similitudes en cuanto a su composición. El presente trabajo describe las petrofacies arenosas desarrolladas durante los dos períodos de rifting. Es posible establecer un total de seis petrofacies: dos relacionadas con el Rift-1 (PT-1 y PT-2) y cuatro con el Rift-2 (JC-1 a JC-4). Todas estas petrofacies pueden ser consideradas bien como sedimentoclásticas o como plutoniclásticas.

Las petrofacies sedimentoclásticas se desarrollaron durante las etapas iniciales de rifting debido al reciclado del registro sedimentario pre-rift, o por importantes cambios paleogeográficos. Aparecen constituyendo sucesiones de depósitos clásticos poco potentes (<100 m) con areniscas cuarzosas y cuarzolíticas maduras con fragmentos de roca sedimentaria y metasedimentaria. La diagénesis está dominada por la presencia de carbonatos sobre los minerales de la arcilla. Esta petrofacies ha sido reconocida durante el ciclo Rift-1 (PT-1, facies saxoniense) y Rift-2 (JC-1 y JC-3; Titoniense y Valanginiense, respectivamente). Además, puede desarrollarse una petrofacies metasedimentoclástica debido a la erosión del sustrato metamórfico de bajo y medio grado, una vez desmantelada la cobertera sedimentaria pre-rift.

Las petrofacies plutoniclásticas se desarrollaron durante los periodos de máxima actividad tectónica asociada a un importante proceso de denudación y erosión de rocas plutónicas en el área fuente. Constituyen registros estratigráficos potentes (1000 a 4000 m) con petrofacies arenosas feldespáticas caracterizadas por un esqueleto rígido y el predominio de una diagénesis protagonizada por los minerales de la arcilla. Durante el ciclo Rift-1, la petrofacies plutonoclástica desarrollada (PT-2) está asociada a las facies Buntsandstein. Durante el ciclo Rift-2, la petrofacies plutoniclástica (JC-4) está representada por las secuencias deposicionales DS-5 a DS-8 (Hauteriviense-Albiense Inferior), constituyendo la etapa principal de relleno de la Cuenca de Cameros.

Las petrofacies sedimentoclásticas y plutoniclásticas analizadas pueden agruparse en tres pares de petrofacies elementales. Cada par representaría un "ciclo de procedencia", abarcando un ciclo detrítico completo de un periodo de rifting. Las petrofacies PT-1 y PT-2 representan el "ciclo de procedencia" durante Rift-1. En la Cuenca de Cameros, y durante el ciclo Rift-2, pueden distinguirse dos "ciclos de procedencia" relacionados con las megasecuencias Titoniense-Berriasiense y Valanginiense-Albiense Inferior.

Por último, la tectónica es el factor principal que controla las petrofacies. No obstante, otros factores (i.e., maduración durante el transporte, aportes locales) pueden modular la señal de la composición de las petrofacies. Sin embargo, el carácter principal de la petrofacies persiste y es capaz de subrayar la jerarquía de las superficies estratigráficas principales de la Cuenca Ibérica de rift intracontinental.

Palabras clave: Procedencia, areniscas, petrofacies, cuencas de rift, Cordillera Ibérica, Permo-Trías, Cretácico Inferior..

1. Introduction

Sandstone petrography is a powerful tool for deciphering both the composition of source terrains (e.g., Basu, 1976; Mack, 1981; Palomares and Arribas, 1993; Arribas and Tortosa, 2003) and the geotectonic setting, in which ancient terrigenous deposits formed (e.g., Dickinson and Suczek, 1979; Dickinson *et al.*, 1983; Dickinson, 1985; Valoni, 1985). Sand composition is also sensitive to other factors involved in the clastic sediment system (Johnsson, 1993), and valuable information about climate, relief and transport can be obtained from the framework composition of sandstones. Actualistic approaches permit a better understanding of the contribution of these factors to sand composition (e.g., Grantham and Velbel, 1988; Johnsson *et al.*, 1991; Ibbeken and Schleyer, 1991; Nesbitt *et al.*, 1997; Critelli *et al.*, 1997; Le Pera and Critelli, 1997). All of this information is crucial for any basin analysis and may help distinguish boundary surfaces and the internal anatomy of unconformity-bounded units of the basin fill (Fontana *et al.,* 1989; Zuffa *et al.*, 1995; Arribas *et al.*, 2003). Thus, petrofacies are useful for analyzing depositional sequences and, consequently, the organization and develop of the clastic sedimentary record of the basin filling.

In marine sediments, where sandstone composition is very sensitive to changes in intrabasinal sources, sea-level changes, etc., this type of study is common. However, relationships between petrofacies and depositional sequences in continental settings have been poorly documented. In this type of setting, tectonics exerts the main control on topography and determines sediment flux from catchments (Prosser, 1993). This flux is, in turn, modulated by the source rock lithologies and climate (Palomares and Arribas, 1993; Leeder, 1995, respectively).

The Iberian Range (Fig. 1) is an intracratonic, folded segment of the Alpine Chain that developed as a rift basin from Permian to late Cretaceous times (Alvaro *et al.*,

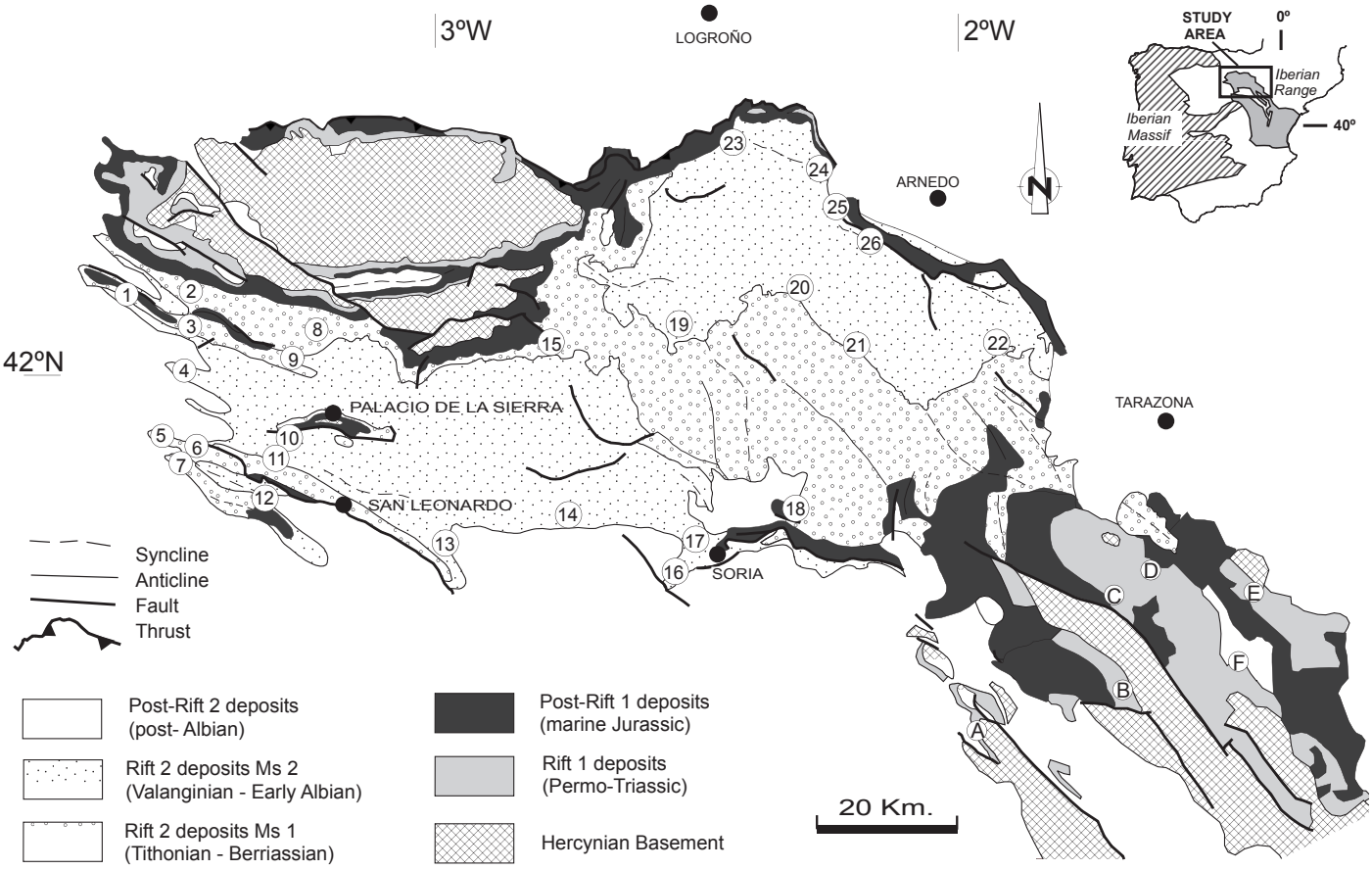

Fig. 1.- Geological map of the northern sector of the Iberian Chain (Cameros Basin and Aragonese Branch) highlighting the distribution of rift and post-rift sediments. Numbers refer to the stratigraphic successions considered in the Cameros Basin (Rift-2). Capital letters refer to the stratigraphic successions considered in the Aragonese Branch (Rift-1). 1: Cubillejas. 2: Rupelo. 3: Campolara. 4: Contreras. 5: Hinojosa. 6: Peñacoba. 7: Arroyo del Helechal. 8: Terrazas. 9: Castrovido. 10: Moncalvillo. 11: La Gallega. 12: Brezales. 13: Talveila-Muriel. 14: Cidones-Abejar. 15: Montenegro. 16: Hoya del Moro. 17: Trinchera del ferrocarril. 18: Almajano. 19: San Andrés. 20: Yanguas. 21: S. Pedro Manrique. 22: Valdemadera. 23: Trevijano. 24: Jubera. 25: Arnedillo. 26: Préjano. A: La Alameda. B: Aranda del Moncayo. C: Beratón. D: Moncayo. E: Tabuenca. F: Tierga.

Fig. 1.- Mapa geológico del sector noroccidental de la Cordillera Ibérica (Cuenca de Cameros y Rama Aragonesa) resaltando la distribución de los depósitos de rift y post-rift. Los números se refieren a las series estratigráficas de la Cuenca de Cameros (Rift-2) consideradas. Las letras mayúsculas se refieren a las series estratigráficas de la Rama Aragonesa (Rift-1) consideradas. 1: Cubillejas. 2: Rupelo. 3: Campolara. 4: Contreras. 5: Hinojosa. 6: Peñacoba. 7: Arroyo del Helechal. 8: Terrazas. 9: Castrovido. 10: Moncalvillo. 11: La Gallega. 12: Brezales. 13: Talveila-Muriel. 14: Cidones-Abejar. 15: Montenegro. 16: Hoya del Moro. 17: Trinchera del ferrocarril. 18: Almajano. 19: San Andrés. 20: Yanguas. 21: S. Pedro Manrique. 22: Valdemadera. 23: Trevijano. 24: Jubera. 25: Arnedillo. 26: Préjano. A: La Alameda. B: Aranda del Moncayo. C: Beratón. D: Moncayo. E: Tabuenca. F: Tierga.

1979; Vilas *et al.*, 1983; Salas and Casas, 1993; Roca *et al.*, 1994; Salas *et al.*, 2001; Mas *et al.*, 2003). The Iberian Basin was filled with thick clastic sequences during two rifting cycles (Salas *et al.*, 2001): the first cycle spanned the Late Permian to Late Triassic, and the second cycle was developed from the Late Jurassic to Early Albian. During these active periods, sedimentation took place mainly in alluvial to lacustrine environments in a complex system of extensional basins. Both cycles evolved to periods of post-rift thermal subsidence where shallow-marine carbonates were deposited. The configuration and development of the Iberian Rift Basin during both active intervals differed markedly, affecting both the characteristics of the clastic record, as well as sandstone composition.

Several authors have examined sandstone composition in continental rift basins, including, Cavazza (1986), Evans (1990), Garzanti *et al.*, (2001), Garzanti *et al.* (2003), Hubert *et al.* (1992), Soreghan and Cohen (1993), and Zuffa *et al.* (1980). This paper documents sandstone petrofacies developed during the two rift stages in the northwestern sector of the Iberian Basin (Fig. 1) (Aragonese Branch of the Iberian Range and the Cameros Basin) and elucidates the main factors controlling sandstone composition in this basin. In addition, we suggest the cyclicity of sandstone composition in the sedimentary record of the northern Iberian Basin.

2. Geological setting

The basins forming part of the Mesozoic Iberian Rift System (Mas *et al.*, 1993; Guimerà *et al.*, 1995; Salas *et al.*, 2001) are located in the northeastern region of Iberia and in its adjacent Mediterranean off-shore region (Fig. 1). These basins contain thick successions of Late Permian and Mesozoic continental and shallow-marine clastics, carbonates and minor evaporites. Sediments overlie the regional Late Variscan unconformity, which truncates folded Palaeozoic sedimentary, metamorphic and intrusive rocks. The Mesozoic sedimentary succession of the Iberian basins shows dramatic lateral changes in thickness from <1000 m to c. 6000 m across distances of few kilometres, suggesting that tectonic activity significantly influence their development.

The Iberian Rift System was inverted during Palaeogene-Early Neogene times to generate the Iberian Chain (Salas *et al.*, 1992; Salas *et al.*, 2001). This chain is a complex NW-SE striking intraplate compressional feature (Fig. 1), where deformation was directly related to the collision of the Iberian craton with Europe during the Pyrenean Orogeny (Guimerà, 1984; Guimerà and Álvaro, 1990) as well as to the contemporaneous early stages of the Betic Orogeny (Vera, 2001).

The course of development of the Iberian Rift System during the Late Permian and Mesozoic has been divided into four major rift cycles and their corresponding post-rift stages (Salas *et al.*, 2001) (Fig. 2). In the NW sector of the Iberian Chain, four megacycles or depositional supersequences, bounded by regional unconformities, have been recognised (Guimerà *et al.*, 2004; Salas *et al.*, 2001) and namely: the Late Permian to Triassic Megacycle 1 (Rift cycle 1); the Early to Late Jurassic Megacycle 2 (post-rift stage 1); the Latest Jurassic to Early Cretaceous Megacycle 3 (Rift cycle 2); and the Late Cretaceous Megacycle 4 (post-rift stage 2) (Fig. 2).

During the Late Permian to Triassic Megacycle 1 (Rift cycle 1; Salas *et al.*, 2001), the development of the Iberian Basin commenced with the extensional reactivation of late-Variscan faults (Vegas and Banda, 1982). As a consequence, Late Permian and Triassic deposits unconformably overlie the Variscan basement and filled a complex halfgraben-graben system (Arche and López-Gómez, 1996). In most of the Iberian Basin, these deposits correspond to continental environments, mainly of alluvial-fluvial character (Buntsandstein facies), that progressively evolved to shallow-marine, coastal carbonate (Muschelkalk facies) and coastal evaporitic environments (Keuper facies). In the NW part of the Iberian Chain, these deposits crop out at the edges of the Demanda Massif north of the Cameros Range, and southeast in the Moncayo area. During the deposition of the Buntsandstein facies, depocenters were located in the southeastern part of the basin (Moncayo area), and here clastic deposits show considerable lateral thickness variations (from 100 m in the SW to more than 900 m towards the NE). In the Moncayo area, and at the base of the stratigraphic succession, red-bed Saxonian facies has been identified (Arribas, 1985). The subsequent Early to Late Jurassic Megacycle 2 (Post-rift stage 1) was mainly dominated by thermal subsidence and the extensive development of carbonate platforms (Salas *et al.*, 2001).

In the NW of the Iberian Chain, the Latest Jurassic to Early Cretaceous Rift cycle 2 (Salas *et al.*, 2001) corresponds to the fill of the Cameros Basin, extending from the Tithonian to the Early Albian, and corresponding to a large cycle bounded at the base and top by two main unconformities (Fig. 2). The sedimentary record of the Cameros Basin is asymmetric, such that the stratigraphic gap related to the lower limit unconformity is more relevant in the northern part of the basin than in central and southern areas. The Latest Jurassic-Early Cretaceous Megacycle 3 can be subdivided into eight depositional sequences bounded by unconformities (Mas *et al.*, 1993; Mas *et al.*, 1997; Martín-Closas and Alonso Millán, 1998; Arribas *et al.*, 2003) (Fig. 2). The sediments are mainly continental, and are usually organized into cycles, which commence with alluvial-fluvial clastics at the base, and change to lacustrine limestones and marls towards the top (Alonso and Mas, 1993; Gómez-Fernández and Meléndez, 1994). Depositional sequences are generally thick and palaeocurrent data suggest that the main siliciclastic source was the Iberian Massif on the SW margin (Mas *et al.*, 1997; Mas *et al.*, 2002-2005; Arribas *et al.*, 2003; Mas *et al.*, 2003).

The upper limit of the Latest Jurassic to Early Cretaceous Megacycle 3 is an intra-Albian unconformity bounding the base of Late Cretaceous Megacycle 4 (Post-rift stage 2; Salas *et al.*, 2001) of the Iberian Chain (Fig. 2). Above this unconformity, the Cameros Basin loses its identity and large carbonate platforms occupy the Iberian realm (Alonso *et al.*, 1989; Alonso *et al.*, 1993), as reported from other Latest Jurassic-Early Cretaceous Iberian rifting basins.

Detailed information concerning the configuration, subsidence and development of the Cameros Basin, as well as diagenesis, petroleum systems and hydrothermal metamorphism within the basin, can be obtained from Casquet *et al.*, 1992; Mas *et al.*, 1993; Alonso-Azcárate *et al.*, 1995; Barrenechea *et al.*, 1995; Guimerà *et al.*, 1995; Mantilla-Figueroa *et al.*, 1998; Alonso-Azcárate *et al.*, 1999; Barrenechea *et al.*, 2000; Alonso-Azcárate *et al.*,

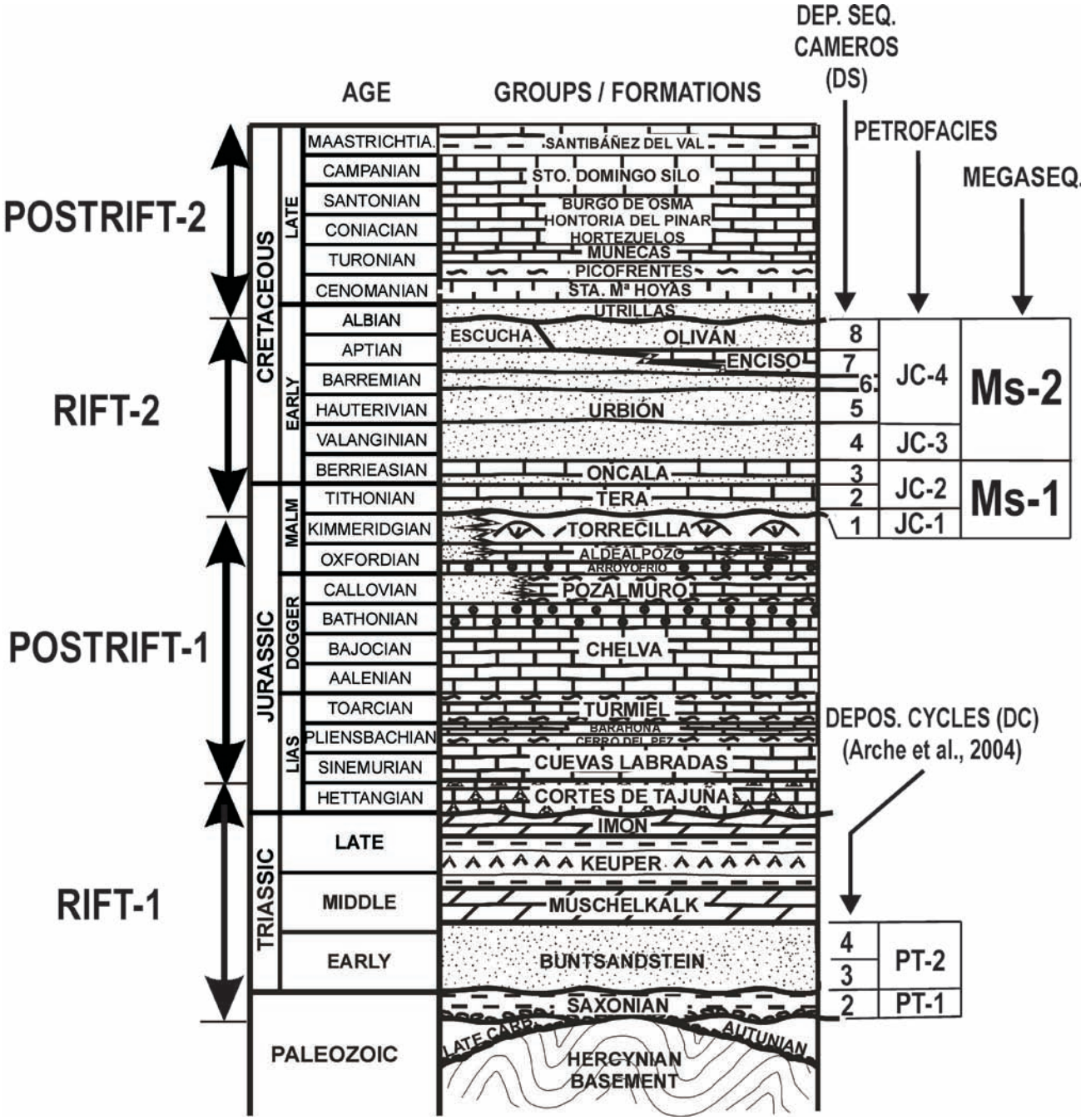

Fig. 2.- Idealized sketch showing the latest Paleozoic and Mesozoic stratigraphic record of the northern sector of the Iberian Chain (modified from Mas *et al.*, 2003). Petrofacies appear along with their stratigraphic intervals: depositional sequences (DS) and megasequences (Ms) in the Cameros Basin (Rift-2), and depositional cycles (Arche *et al.*, 2004) in the Aragonese Branch (Rift-1).

Fig. 2.- Esquema idealizado mostrando la sucesión estratigráfica del registro superior del Paleozoico y del Mesozoico del sector noroccidental de la Cordillera Ibérica (modificado de Mas *et al.*, 2003). Asimismo se muestran las distintas petrofacies asociadas a su intervalo estratigráfico: Secuencias deposicionales (DS) y megasecuencias (Ms) en la Cuenca de Cameros (Rift-2) y ciclos deposicionales (Arche *et al.*, 2004) en la Rama Aragonesa (Rift-1).

2001; Mantilla-Figueroa *et al.*, 2002-2005; Mas *et al.*, 2003; and Mas *et. al* 2002-2005; Ochoa *et al.*, 2005.

3. Methodology

This paper summarizes the results of previous petrographic studies of Permo-Triassic and Upper Jurassic-Early Cretaceous sandstones of the Aragonese Chain and the Cameros Basin, respectively (Arribas, 1984; Arribas *et al.*, 1985; Arribas *et al.*, 2003; Ochoa *et al.*, 2004; Ochoa *et al.*, 2005; González *et al.*, 2005). The petrographic databases from these papers were examined and re-evaluated for a homogeneous treatment of the data. We reviewed data from more than three-hundred samples ob-

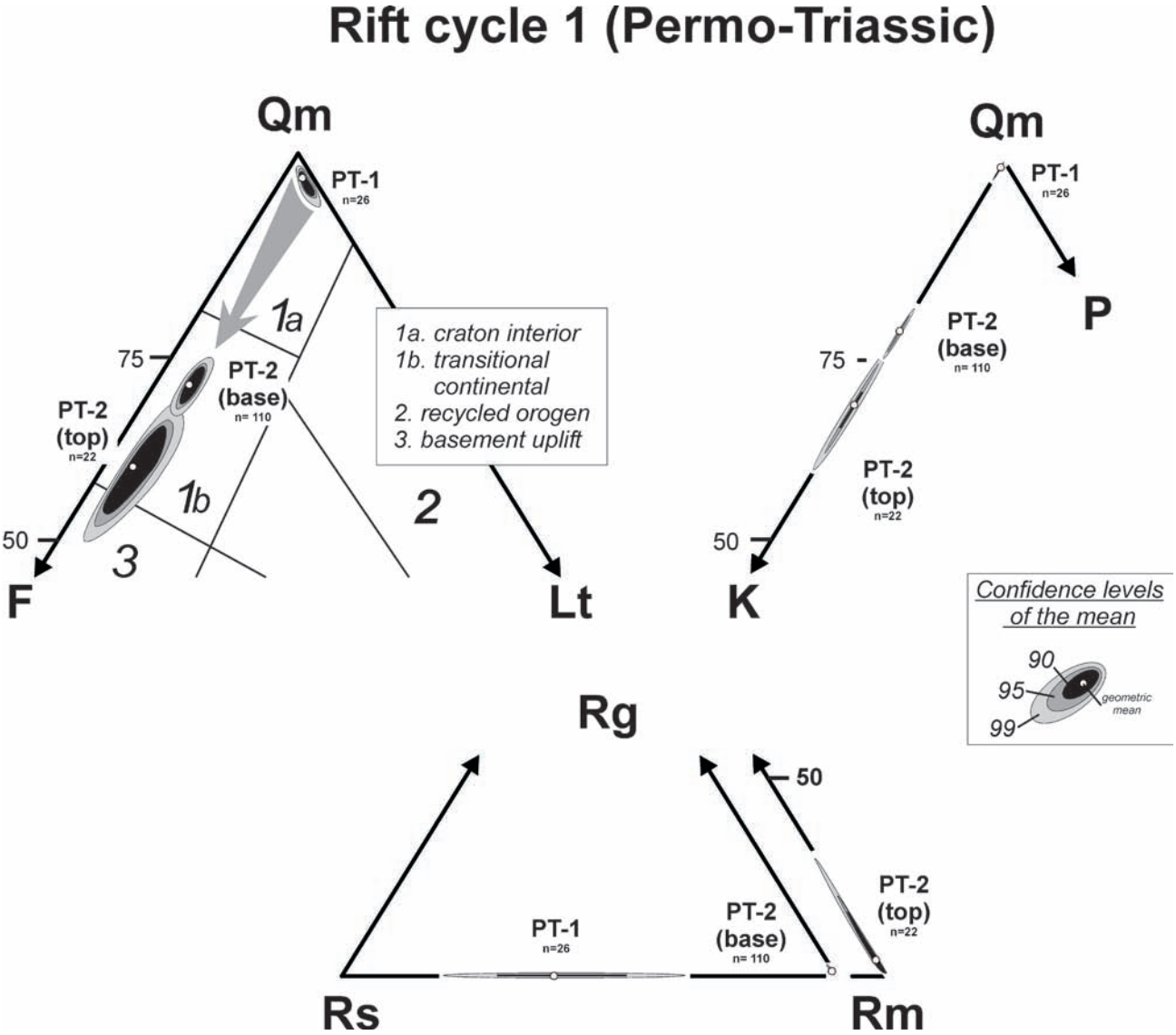

Fig. 3.- Compositional diagrams of the sandstone framework (QmFLt, QmKP from Dickinson *et al.*, 1983; and RgRsRm from Arribas *et al.,* 1990; and Critelli and Le Pera, 1994) that describes the petrofacies of Rift cycle 1 (PT-1 and PT-2). Areas of confidence levels of the mean were calculated according to the procedure described by Weltje (2002).

Fig. 3.- Diagramas composicionales del esqueleto de areniscas (QmFLt, QmKP de Dickinson *et al.*, 1983; y RgRsRm de Arribas *et al.,* 1990; y Critelli y Le Pera, 1994) que describen las petrofacies del Rift-1 (PT-1 y PT-2). Las áreas correspondientes a los niveles de confidencia de la media se han obtenido siguiendo los métodos propuestos por Weltje (2002).

tained by point counting (400 to 500 points) performed on the corresponding thin sections, using the 'Gazzi-Dickinson method' (Ingersoll *et al.*, 1984) according to the petrographic groups defined by Zuffa (1980). This procedure permits a re-evaluation of framework composition according to the 'traditional' method (Pettijohn, 1957). In addition, by re-evaluating petrographic data taking diagenetic alterations (e.g. epimatrix, pseudomatrix, dissolution of framework grains) into account, the original framework composition of the sediment can be restored. Key indices for framework composition were used to plot samples in diagnostic provenance diagrams as QmFLt and QmKP (Dickinson *et al.*, 1983) and RgRsRm (Arribas *et al.*, 1990; Critelli and Le Pera, 1994). Confidence regions about the mean (90%, 95% and 99%) were calculated following the rigorous statistical methods proposed by Weltje (2002). Thin sections were prepared using classic procedures including: (1) impregnation with blue epoxy resin before thin-section grinding, and (2) selective staining and etching for feldspars and carbonate identification. All these procedures are described in detail in the original papers cited above.

4. Results

4.1. Rift cycle 1 (Permo-Triassic)

Sandstone compositions of Permo-Triassic deposits from the Moncayo area in the Iberian Range have been previously reported (Arribas, 1984; Arribas, 1985; Arribas *et al.*, 1985; Arribas, 1987). Permo-Triassic sandstones were initially deposited in a continental environment that evolved to transitional environments at the top (Arribas, 1985). The framework composition of sandstones varies from quartzose at the base of the succession (Saxonian facies) to quartzofeldspathic at the top of the sedimentary sequence (Buntsandstein facies), and two sets of petrofacies can be defined.

Petrofacies PT-1. This is a quartzose petrofacies (mean $Qm_{97}F_{0}Lt_{3}$, Fig. 3) that characterizes the base of the Permo-Triassic succession (Saxonian facies). This petrofacies is found in thin channelized and non-channelized sandstone beds (<3 m) in association with orthoquartzitic conglomerates, and it is interbedded with silty-clayed deposits which show evidence of palaeosoil development. These deposits have all been interpreted in the context of an alluvial fan system (Arribas, 1985). The sandstone petrofacies is very mature, showing clear sorting and high quartz grain roundness values (Fig. 4A). Non-undulose monocrystalline quartz is the main quartz grain type present (mean $Qmr_{60}Qmo_{21}Qp_{19}$). Lithic rock fragments are scarce (mean 3%) and correspond to low-grade metasediments (mainly shales and chert) (Fig. 3). Some quartzose sandstone fragments and quartz grains with abraded inherited quartz cement have also been identified. The framework was affected by intense chemical compaction processes manifested by the presence of concavo-convex and sutured grain contacts. This compaction may be the reason for the relatively high contents of the Qmo quartz grains (Graham *et al.*, 1976; Arribas *et al.*, 1985). Intergranular volume is low, and pore space is nearly entirely occupied by quartz overgrowth (Fig. 4A). The clay matrix is negligible and only appears locally as a product of the desegregation of silty-clay grains (pseudomatrix).

Petrographic features reflect maturation during transport and the recycling of low-grade metasediments (metasandstones and shales) from the Variscan basement. Saxonian sandstones display a very homogeneous framework composition across the Moncayo area and represent the initial stage of Rift-1, coeval with erosion of the metasedimentary basement. In a QmFLt diagram, sandstones from this petrofacies plot within the 'stable craton' field (Dickinson *et al.*, 1983) close to the Qm-Lt edge (Fig. 3). Thus, the sedimentoclastic quarzose nature of this petrofacies suggests intense maturation from a previous sedimentolithic petrofacies. The denudation regime can therefore be considered as transport-limited (Johnsson, 1993).

Petrofacies PT-2. This quartzofeldspathic petrofacies (mean $Qm_{72}F_{25}Lt_{3}$, Fig. 4) characterizes the sandstones of the Buntsandstein facies (Fig. 4B). Thick (>20 m) channelized and amalgamated sandstone bodies commonly appear at the base of Buntsandstein facies and were generated in a low-sinuosity fluvial system. At the top of the succession, sandstones bodies occur as isolated channels and non-channelized bodies interbedded with silts and clays deposits. This part of the succession is interpreted as a fluvial system of greater sinuosity and distality. Quartz grains include both monocrystalline and polycrystalline typologies (mean $Qmr_{56}Qmo_{18}Qp_{26}$) as well as chert. Feldspar is mainly K-feldspar (microcline and orthoclase), with trace amounts of plagioclase. K-feldspar increases considerably towards the top of the succession (Fig. 3). Lithic rock fragments are common and appear as labile fine-grained clasts (shales) and chert grains. Coarse-grained rock fragments (plutonites) are also frequent. Diagenetic framework changes include mechanical and, to a lesser extent, chemical compaction. Cements are widespread and consist mainly of quartz and K-feldspar overgrowths and carbonate mosaics. Secondary porosity involves K-feldspar and carbonate cement dissolution. Diagenetic matrix appears as epimatrix (K-feldspars replaced by illite and kaolinite), pseudomatrix (breaking up of lithic fragments), kaolinite pore-filling and illite pore-lining (Arribas, 1987). In many cases, sandstones contain high proportions (>15%) of diagenetic matrix (arkosic wackes).

The quartzofeldspathic petrofacies represents a significant change in both composition and provenance from the underlying sediments. This petrofacies suggests a dominant first-order supply from coarse crystalline rocks (plutonites) from the Variscan basement during Buntsandstein sedimentation. The increase in K-feldspar content over time suggests the progressive dominance of coarse-grained supplies over low-grade metasedimentary ones. Low-grade metasedimentary rocks always appear as source terrains, but their sandy products are gradually diluted by the great sand generation potential that plutonites have (Palomares and Arribas, 1993). K-feldspar rich petrofacies are indicative both of the arid conditions under which Buntsandstein sedimentation developed (Arribas, 1984) as well as the closeness of source areas. Sandstones plot in the 'transitional continental' to 'basement uplift' fields in the QmFLt diagram (Fig. 3). This petrofacies was generated during a period of maximum basin

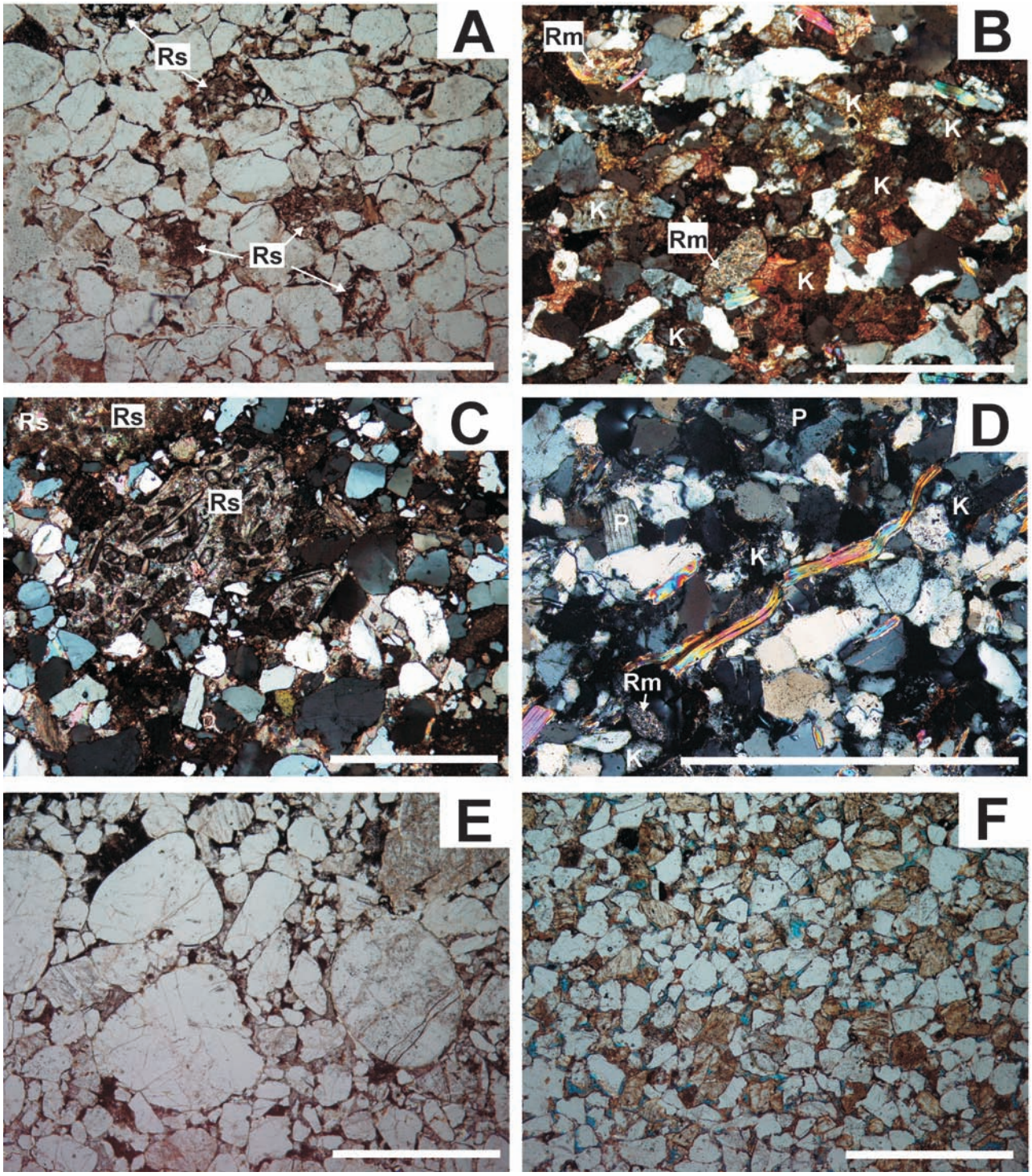

Fig. 4.- Thin section photomicrographs of sandstone petrofacies from the northern sector of the Iberian Basin. **A**) Quartzose sedimentoclastic petrofacies PT-1 showing siliciclastic (sandstones and siltites) rock fragments (Rs). Plane-polarized light. **B**) Quartzofeldspathic (plutoniclastic) petrofacies PT-2 showing abundant K-feldspar grains (K) and the presence of low-grade metamorphic rock fragments (Rm). Cross-polarized light. **C**) Sedimentoclastic petrofacies JC-1 showing sedimentary carbonate rock fragments (from marine Jurassic formations). Note the dominance of rounded monocrystalline quartz grains and the presence of carbonate cement. Cross-polarized light. **D**) Quartzofeldspathic (metasedimentoclastic) petrofacies JC-2 characterized by the presence of plagioclase (P) and K-feldspar (K) grains with mica and low-grade metamorphic rock fragments (Rm). Cross-polarized light. **E**) Quartzose (sedimentoclastic) petrofacies JC-3 showing the dominance of rounded quartz grains. Intergranular spaces occupied by carbonate cement. Plane-polarized light. **F**) General view of quartzofeldspathic (plutoniclastic) petrofacies JC-4. Note the great abundance of K-feldspar grains (dark grains) and scarce roundness of quartz grains. Plane-polarized light. Scale bar in all photographs is 1 mm.

subsidence and high tectonic activity and corresponds to the main stage of rifting. This stage is characterized by a weathering-limited denudation regime (Johnsson, 1993) promoted by an arid climate. Spatial variation in sandstone composition was not observed, and this is attributable to the narrowness of the troughs which prevented sediment maturation during transport.

4.2. Rift cycle 2 (Late Jurassic – Early Cretaceous)

The sedimentary record of the Cameros Basin during the most active period of rifting (Late Jurassic-Early Cretaceous) can be subdivided in two megasequences (Tithonian-Berriasian, and Valanginian-Early Albian) including three and five depositional sequences (DS, Fig. 2), respectively (Salas *et al.*, 2001; Mas *et al.*, 2003). The petrographic characterization of the sandstones can be found in Arribas *et al.* (2003), Ochoa *et al.*, (2004) Arribas *et al.* (2002-2005), González *et al.* (2005), Najarro (2005) and Najarro *et al.* (2005). Two different petrofacies can be distinguished in each megasequence.

4.2.1. Megasequence 1 (Tithonian - Berriasian)

Petrofacies JC-1. This petrofacies is quartzolithic (mean $Qm_{83}F_3Lt_{14}$), and developed during the sedimentation of DS-1. Sandstones are quartzarenites and sedarenites containing variable amounts of carbonate rock fragments (Fig. 4C). Well-rounded monocrystalline quartz dominates ($Qmr_{60}Qmo_{28}Qp_{12}$). Other siliciclastic grains include K-feldspar, plagioclase and metamorphic lithic, appearing in low proportions. Carbonate rock fragments dominate the lithic population. These are variable both in their textures and composition. Intrabasinal carbonate grains are also common. The main postdepositional modifications include mechanical and chemical compaction and carbonate cementation.

This petrofacies represents the recycling of the prerift sedimentary cover (mainly carbonate marine Jurassic deposits) during the first stage of Rift-2. In the areas of maximum subsidence, additional supplies from low-grade metamorphic rocks (fine-grained schists and slates) are also recorded at the top of the sequence. Sandstone samples plot near the QmLt edge (Fig. 5) within the 'recycled orogen' field of Dickinson *et al.* (1983), evidencing the sedimentoclastic origin of this petrofacies.

Petrofacies JC-2. This quartzofeldspathic petrofacies (mean $Qm_{84}F_{12}Lt_4$) developed during the sedimentation of DS-2 and DS-3, and is present in the SW area of the Cameros Basin. Sandstones are subarkoses (Fig. 4D) with albite (twinned and untwinned grains) and K-feldspar grains. Substantially higher amounts of polycrystalline quartz are observed (mean $Qmr_{48}Qmo_{17}Qp_{35}$) compared to the previous petrofacies. The rock fragment population is dominantly comprised of metamorphic lithics (slates and micaschists) and rare sedimentary lithic fragments (carbonates). Other siliciclastic grains include micas (muscovite, biotite), dense minerals and silty rip-up clasts. A gradual decrease in the content of sedimentary lithics towards the top of the sequence is also apparent. Thus, at the top of the DS-3 sequence the rock fragment population is solely made up of low-grade metamorphics. Quartz and feldspar overgrowths are common. A clay matrix is common and includes kaolinite pore filling and replacements.

The petrographic characteristics of the sandstone framework indicate that this petrofacies was mainly derived from low-grade to medium-grade metamorphic and minor sedimentary terrains. In addition, supplies from sedimentary rocks tend to disappear towards the top of the sequence. Sandstones plot in the transitional provenance field (Fig. 5) between the 'basement uplift' and 'stable craton' fields (Dickinson *et al.*, 1983). Sources are related to the Variscan basement (Asturian-Leonese Zone) and the remains of sedimentary rocks from the marine Jurassic pre-rift cover.

4.2.2. Megasequence 2 (Valanginian - Early Albian)

Petrofacies JC-3. The distribution of this petrofacies is very restricted and coincides with the sedimentation of DS-4 in the southwest area of the Cameros Basin. It is a quartzose petrofacies (mean of $Qm_{95}F_3Lt_2$, Fig. 6) comprised mainly of quartzarenites and minor amounts of subarkoses (Fig. 4E). The quartz population is characterized by the presence of rounded grains, with a predominance

Fig. 4 (página anterior).- Fotografías de láminas delgadas de las petrofacies arenosas del sector noroccidental de la Cuenca Ibérica. **A**) Petrofacies cuarzosa sedimentoclástica PT-1 mostrando fragmentos de rocas sedimentarias siliciclásticas (areniscas y lutitas aleuríticas) (Rs). Nícoles paralelos. **B**) Petrofacies cuarzofeldespática (plutoniclástica) PT-2 con abundancia de feldespatos potásicos (K) y fragmentos de roca metamórfica de bajo grado (Rm). Nícoles cruzados. **C**) Petrofacies sedimentoclástica JC-1 donde se observan fragmentos de roca carbonática (de formaciones del Jurásico marino). Notar el dominio de granos de cuarzo monocristalino con elevada redondez y la presencia de cemento carbonático. Nícoles cruzados. **D**) Petrofacies cuarzofeldespática metasedimentoclástica JC-2 caracterizada por la presencia de granos de plagioclasa (P) y feldespato potásico (K) con micas y fragmentos de roca metamórfica de bajo grado (Rm). Nícoles cruzados. E) Petrofacies cuarzosa (sedimentoclástica) JC-3 donde se observa el dominio de granos de cuarzo redondeados. El espacio intergranular se encuentra ocupado por cemento carbonático. Nícoles paralelos. **F**) Vista general de la petrofacies cuarzofeldespática (plutoniclástica) JC-4. Notar la abundancia de feldespato potásico (granos oscuros) y la baja redondez de los granos de cuarzo. Nícoles paralelos. La escala gráfica en todas las fotografías es 1 mm.

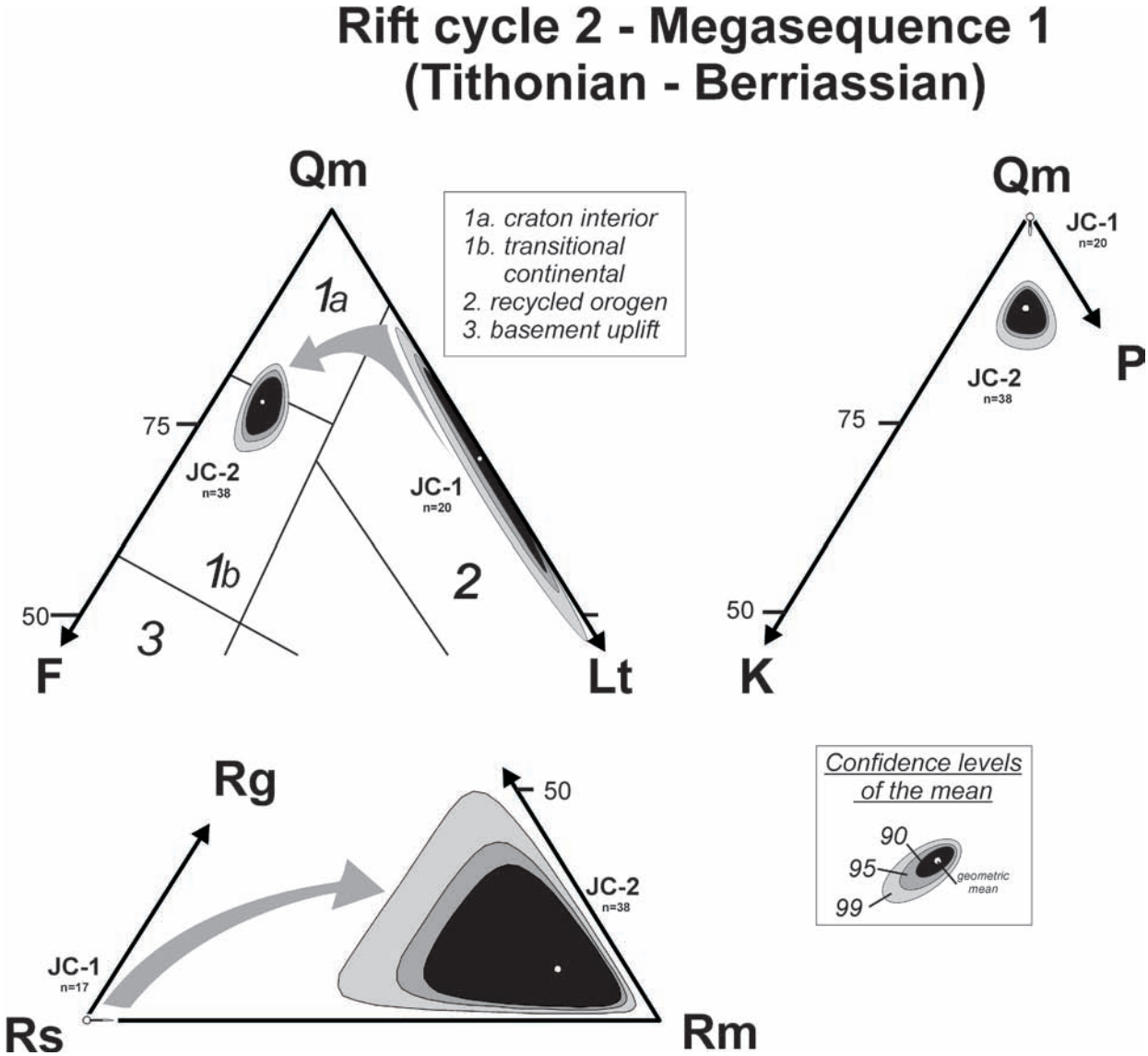

Fig. 5.- Compositional diagrams of sandstone framework (QmFLt, QmKP from Dickinson *et al.*, 1983; and RgRsRm from Arribas *et al.,* 1990; and Critelli and Le Pera, 1994) describing petrofacies from megasequence 1 in Rift cycle 2 (JC-1 and JC-2). Areas of confidence levels of the mean were calculated according to the procedure described by Weltje (2002).

Fig. 5.- Diagramas composicionales del esqueleto de areniscas (QmFLt, QmKP de Dickinson *et al.*, 1983; y RgRsRm de Arribas *et al.,* 1990; y Critelli y Le Pera, 1994) que describen las petrofacies correspondientes a la megasecuencia 1 del Rift-2 (JC-1 y JC-2). Las áreas correspondientes a los niveles de confidencia de la media se han obtenido siguiendo los métodos propuestos por Weltje (2002).

of monocrystalline types (mean of $Qmr_{63}Qmo_{25}Qp_{12}$). Abraded quartz overgrowths are frequent. The feldspar population is exclusively composed of K-feldspar grains. Lithic grains are scarce and consist mainly of sedimentary carbonate grains. Metamorphic lithics are rare. Soft intrabasinal carbonate grains also appear. These sandstones are commonly cemented by the early phases of kaolinite and dolomite, avoiding the effects of framework compaction.

Many of the petrographic features observed suggest that this petrofacies is the result of recycling processes from sedimentary rocks, in accordance with plots in the 'stable craton' field (Fig. 6) of Dickinson *et al.* (1983). Older Jurassic and Triassic sedimentary rocks (mainly carbonates, arkoses and shales) have been suggested as the main potential sources for this petrofacies (Arribas *et al.*, 2003).

Petrofacies JC-4. This petrofacies is widely distributed throughout the Cameros Basin and from DS-5 to DS-8. It is a quartzofeldspathic petrofacies (Figs. 4F and 6) displaying significant compositional variation (from quartzarenites to arkoses). In the southwestern part of the basin (10, 11, 13, 14 and 17 in Fig.1), feldspar contents increase from the older to younger depositional sequences. In addition, spatial variation in composition is manifested in

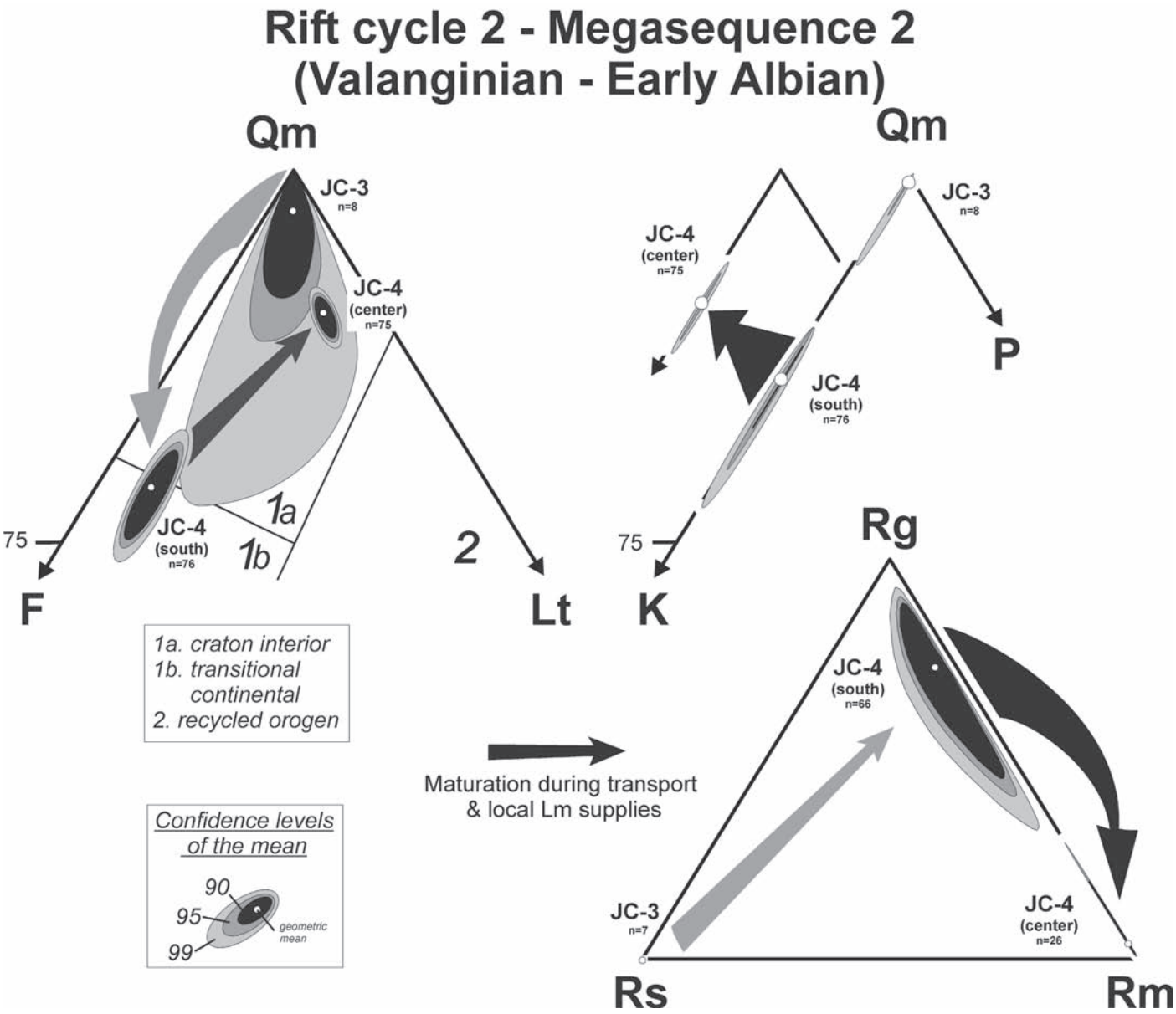

Fig. 6.- Compositional diagrams of a sandstone framework (QmFLt, QmKP from Dickinson *et al.*, 1983; and RgRsRm from Arribas *et al.,* 1990; and Critelli and Le Pera, 1994) describing petrofacies from megasequence 2 in Rift cycle 2 (JC-3 and JC-4). Areas of confidence levels of the mean were calculated according to the procedure described by Weltje (2002). Black arrows represent composition changes due to maturation and local supplies in petrofacies JC-4. See text for more details.

Fig. 6.- Diagramas composicionales del esqueleto de areniscas (QmFLt, QmKP de Dickinson *et al.*, 1983; y RgRsRm de Arribas *et al.,* 1990; y Critelli y Le Pera, 1994) que describen las petrofacies correspondientes a la megasecuencia 2 del Rift-2 (JC-3 y JC-4). Las áreas correspondientes a los niveles de confidencia de la media se han obtenido siguiendo los métodos propuestos por Weltje (2002). Las flechas negras representan la evolución de la composición por maduración durante el transporte y por aportes locales en la petrofacies JC-4. Ver texto para mayor información.

DS-7, from feldspathic rich sandstones in the southwest (13, 14 and 17 in Fig. 1) to quartzose sandstone in the northeast (15, 19 to 22 in Fig.1). The framework grains are medium- to coarse-grained and are mainly quartz (mean of $Qmr_{48}Qmo_{22}Qp_{30}$) and feldspar. K-feldspar dominates over plagioclase, with P/F values that change from 0.24 in DS-5 to 0.19 (DS-6) and 0.03 (DS-7). Low-grade metamorphic lithic fragments are rare, but concentrated in the north of the basin and in the uppermost depositional sequences (DS-7 and 8). Coarse-grained rock fragments are also present and consist of phaneritic crystalline quartz-feldspar grains. These are most commonly found in DS-7. Other common accessory grains include micas, argillaceous rip-up clasts and dense minerals. The main diagenetic processes include compaction, manifested by the ductile deformation of soft grains, ex-

tensive rigid grain fracture, collapse-framework features and pressure solution processes between quartz grains. Diagenetic kaolinite is very common, appearing as a pore filling cement and as replacement on feldspar grains (epimatrix). Quartz and K-feldspar overgrowths are not well developed and carbonate cementation is nearly absent. Despite these processes, primary and secondary porosity (mainly K-feldspar dissolution) is preserved (mean of 9.4). In the depocentre of the basin, a low-grade metamorphic event (hydrothermalism) took place, leading to some mineralogical changes in the original petrofacies, including silicification, chloritization and the albitization of feldspars.

This petrofacies developed during the most active rifting phase and characterizes a thick pile of clastic sediments (> 4000 m). Quartzofeldspathic petrofacies are indicative of a first-cycle plutoniclastic origin (Dickinson *et al.,*1983). This evidence is apparent from the base of DS-5, and appears in association with low-grade metamorphic supplies. These supplies were gradually diluted by the former during the sedimentation of successive depositional sequences, as revealed by the decrease in Lm grains and the P/F ratio. Coarse crystalline rocks from the Central Iberian Zone in the Hesperian Massif have been proposed as the principal source for this petrofacies (Arribas *et al.*, 2003). Spatial changes in the composition of the DS-7 petrofacies are related to maturation during transport. The wide configuration of the basin and the humid climate clearly favored the maturation of sediments by weathering and transport towards the main depocentres (Ochoa *et al.*, 2004). However, the increase in Lt from south to north (Fig. 6) can be related to local low-grade metamorphic sources connected to the inner parts of the basin. A transport-limited denudation regime (Johnsson, 1993) could be suggested even if sedimentation took place during high tectonic activity.

At the northern margin of the Cameros Basin (23 to 26 in Fig. 1), Ochoa *et al.* (2004) document a quartzosedimentolithic petrofacies coeval with the deposition of DS-7. This petrofacies was generated by the erosion of the underlying marine Jurassic, and probably also Triassic, deposits located on this passive basin margin. These deposits were not considered in this paper because of their scarce geographic extent and local occurrence.

5. Discussion and concluding remarks

The framework composition of sandstones in clastic deposits from the Iberian Rift shows that the sedimentary record can be divided into several 'provenance cycles' according to the observed petrofacies. These cycles can be correlated with the main events affecting the basin evolution. Tectonic activity is the main factor controlling sedimentation in intracratonic rift basins (Prosser, 1993). Such basins mainly contain a clastic sedimentary infill generated by the erosion of basin margin uplifts, as a result of lithospheric extension. The composition of clastic sediments is highly dependent on the nature of the basement, but modulated by tectonic activity and climate conditions that define the denudation regime (Johnsson, 1993). Other sources (e.g., marine intrabasinal, Zuffa, 1991, among others) and other allocyclic controls (e.g., sea-level changes; Posamentier and Vail, 1988) have a low or negligible impact on sandstone composition. Thus, sandstone composition and petrofacies are sensitive to changes in interior source regions and their evolution over time (e.g., Ingersoll, 1978, 1983, 1990) and can be used to characterize and define depositional sequences and their hierarchy. Two main types of petrofacies have been recognized from the Iberian Basin rifting: (1) sedimentoclastic petrofacies and (2) plutoniclastic petrofacies.

5.1. Sedimentoclastic petrofacies

Sedimentoclastic petrofacies are well developed in the Iberian Basin in cycles Rift-1 and Rift-2. During Permo-Triassic times (Rift-1), a sedimentoclastic petrofacies developed at the base of the sequence (Saxonian facies). This petrofacies (Petrofacies PT-1) is characterized by its metasedimentary provenance. Furthermore, during Rift-2, sedimentoclastic petrofacies were generated. Thus, petrofacies JC-1 and JC-3 developed during the sedimentation of DS-1 (Tithonian) and DS-4 (Berriasian-Valanginian), respectively. The presence of these petrofacies precedes important periods of tectonic activity and forms the base of thick clastic successions (e.g., Salas *et al.*, 2001; Arribas *et al.*, 2003; Mas *et al.* 2002-2005).

Sedimentoclastic petrofacies developed during the initial stages of rifting as a result of recycling from pre-rift sediments deposited over the basement. Mature quartzose and quartzolithic sediments with carbonate clastics occur, and carbonate diagenesis is more common than clay mineral diagenesis. This petrofacies is recorded in a relatively thin succession of sediments (<100 m) characterizing the initial depositional sequence of the basin infill. Garzanti *et al.* (2001) consider this petrofacies to be related to an 'undissected stage' of a rift-shoulder provenance. Other authors such as Zuffa *et al.* (1980) and Evans (1990) observed that sedimentoclastic deposits occur at the beginning of sedimentation in a rifted continental margin. In addition, sedimentoclastic petrofacies may appear throughout the sedimentary record of rift basins, reflecting substantial palaeogeographical changes, involv-

ing new active faults during the propagation of fractures when rifting ensues (Arribas *et al.*, 2003).

Metasedimentoclastic petrofacies may also occur as a product of the erosion of the low- to medium-grade metamorphic substratum of the basin, after the sedimentary cover has been eroded. This intermediate petrofacies can be interpreted as quartzofeldspathic with plagioclase dominant over K-feldspar, and with a high metamorphic lithic content. This petrofacies (JC-2, Fig. 2) was developed during Rift-2 at DS-2 and DS-3 in the Cameros Basin and characterizes a sedimentary sequence almost 400 m thick. Similar petrofacies have been described from the Arabian Sea margin (Garzanti *et al.*, 2001), and they have been considered as a product of an 'undissected-transitional stage' of rift-shoulder provenance.

5.2. Plutoniclastic petrofacies

Plutoniclastic petrofacies are well developed during the period of Buntsandstein sedimentation (Rift-1, Petrofacies PT-2) and during the sedimentation of DS-5 to DS-7 in the Cameros Basin (Rift-2, Petrofacies JC-4) (Fig. 2). The sedimentary record of these petrofacies exceeds 900 m in Rift-1 and 4000 m in Rift-2. In addition to crystalline products, low-grade metamorphic supplies were provided during Buntsandstein sedimentation. These last products are also present in Rift-2 in the inner parts of the basin. Intense weathering led to maturation of sediments during transport toward the NE. According to the denudation regime, the composition of this petrofacies varies from immature feldspar-rich petrofacies in a weathering-limited regime (PT-2 and JC-4 in the SW of Cameros Basin) to mature quartzose petrofacies in a transport-limited regime (JC-4 in the NE of Cameros Basin).

Plutoniclastic petrofacies developed during periods of high tectonic activity. This activity produces high erosional rates on graben and semigraben shoulders, generating sediments from metamorphic and crystalline sources. Quartzofeldspathic petrofacies with low amounts of lithics, a rigid framework and clay mineral diagenesis with slight carbonate cements, are the main compositional features of these first-cycle sediments. The increasing dilution of metamorphic supplies by crystalline-derived sediments can be attributed to the great sand-generating capacity of plutonites (Palomares and Arribas, 1993). In fact, thick piles of plutoniclastic sediments are generated in transport- or weathering-limited regimes according to the climatic conditions. This petrofacies corresponds to the 'dissected stage' of rift-shoulder provenance described by Garzanti *et al.* (2001).

The geotectonic development of intracratonic rifts includes several stages of attenuation and subsequent reactivation of tectonic activity, rendering mature and non-mature sediments, respectively.

Hence, petrofacies concur with the hierarchy of the main bounding surfaces between depositional sequences and highlight the importance of sediment production in each depositional sequence. A 'provenance cycle' including both sedimento- and plutoniclastic petrofacies may define a complete clastic cycle of a rifting stage, from an initial stage to the completion of this rifting stage. This succession of petrofacies has also been observed in other ancient and modern rift basin deposits (e.g., Zuffa *et al.*, 1980; Garzanti *et al.*, 2003).

Acknowledgements

This study was supported by projects DGICYT BTE2001-026 and CGL2005-07445-C03-02/BTE. The manuscript benefited from critical reviews by Tom McCann and an anonymous referee.

References

Alonso, A., Aurell, M., Mas, R., Meléndez, A., Nieva, S., (1989): Estructuración de las plataformas del Jurásico superior en la zona de enlace entre la Cuenca Ibérica y el Estrecho de Soria. In: *XII Congreso Español de Sedimentología*. *Comunicaciones,* Bilbao, 175-178.

Alonso, A., Mas, R., (1993): Control tectónico e influencia del eustatismo en la sedimentación del Cretácico inferior de la cuenca de los Cameros, España. *Cuadernos de Geología Ibérica*.17: 285-310.

Alonso, A., Floquet, M., Mas, R., Meléndez, A., (1993): Late Cretaceous Carbonate Platforms: Origin and Evolution. Iberian Range. Spain. In: T. Simò, R.W. Scott and J.P. Masse (eds.): Cretaceous Carbonate Platforms. *American Association of Petroleum Geologists Memoir,* 56: 297-316.

Alonso-Azcarate, J., Barrenechea, J.F., Rodas, M., Mas, R. (1995): Comparative study of the transition between very low grade metamorphism and low grade metamorphism in siliciclastic and carbonate sediments. Early Cretaceous, Cameros Basin (North Spain). *Clay Minerals*, 30: 407-419.

Alonso-Azcarate, J., Rodas, M., Bottrell, S.H., Raiswell, R., Velasco, F., Mas, R. (1999): Pathways and distances of fluid flow during low grade metamorphism: evidence from pyrite deposits of the Cameros Basin, Spain. *Journal of Metamorphic Geology*, 17: 4, 339-348.

Alonso-Azcarate, J., Rodas, M., Fernández-Díaz, L., Bottrell, S.H., Mas, J. R., López-Andrés, S. (2001): Causes of variation in crystal morphology in metamorphogenic pyrite deposits of the Cameros basin (N Spain). *Geological Journal*, 36: 159-170.

Alvaro, M., Capote, R., Vegas, R. (1979): Un modelo de evolución geotectónica para la Cadena Celtibérica. *Acta Geológica Hispanica*, 14: 172-181.

Arche, A., López-Gómez, J. (1996): Origin of the Permian-Triassic Iberian Basin, central eastern Spain. *Tectonophysics*, 266: 443-464.

Arche, A., López-Gómez, J., Marzo, M., Vargas, H. (2004): The siliciclastic Permian-Triassic deposits in Central and Northeastern Iberian Peninsula (Iberian, Ebro and Catalan Basins): A proposal for correlation. *Geologica Acta*, 2: 305-320.

Arribas, J. (1984): *Sedimentología y diagenesis del Buntsandstein y Muschelkalk de la rama aragonesa de la Cordillera Ibérica (provincias de Soria y Zaragoza)*. Tesis Doctoral, Universidad Complutense de Madrid, 354 p.

Arribas, J. (1985): Base litoestratigráfica de las facies Buntsandstein y Muschelkalk en la rama aragonesa de la Cordillera Ibérica (Zona Norte). *Estudios geológicos*, 41: 47-57.

Arribas, J. (1987): Origen y significado de los cementos en las areniscas de las facies Buntsandstein (Rama Aragonesa de la Cordillera Ibérica). *Cuadernos de Geología Ibérica*, 11: 535-556.

Arribas, J., Marfil, R., de la Peña, J. A. (1985): Provenance of Triassic Feldespathic sandstones in the Iberian Range (Spain): Significance of Quartz types. *Journal of Sedimentary Petrology*, 55: 864–868.

Arribas, J., Gómez-Gras, D., Rosell, J., Tortosa, A., (1990): Estudio comparativo entre las areniscas Paleozoicas y Triásicas de la Isla de Menorca: Evidencias de procesos de reciclado. *Revista de la Sociedad Geológica de España*, 3: 105–116.

Arribas, J., Tortosa, A. (2003): Detrital modes in sedimentoclastic sands from first-order streams of the Iberian Range, Spain: The potential for sand generation of different sedimentary rocks. *Sedimentary Geology*, 15: 275-303.

Arribas, J., Alonso, A., Mas, R., Tortosa, A., Rodas, M., Barrenechea, J. F., Alonso-Azcárate, J., Artigas, R. (2003): Sandstone petrography of continental depositional sequences of an intraplate rift basin: Western Cameros Basin (North Spain). *Journal of Sedimentary Research*, 73 (2): 309-327.

Arribas, J., Ochoa, M., Mas, R. (2002-2005): Composición y diagénesis del registro detrítico en el borde suroccidental de la Cuenca de Cameros. *Zubía*, 14: 99-109.

Barrenechea, F.J., Rodas, M., Mas, J.R. (1995): Clay mineral variation associated to diagenesis and low grade metamorphism of early Cretaceous sediments in the Cameros basin, Spain. *Clay Minerals*, 30: 89-103.

Barrenechea, J.F., Rodas, M., Frey, M., Alonso-Azcarate, J., Mas, J. R. (2000): Chlorite, Corrensite, and Chlorite-Mica in Late Jurassic Fluvio-Lacustrine sediments of the Cameros Basin of Northeastern Spain. *Clays and Clays Minerals*, 48 (2): 256-265.

Basu, A. (1976): Petrology of Holocene fluvial sand derived from plutonic source rocks: implications to paleoclimatic interpretation. *Journal of Sedimentary Petrology*, 46: 694-709.

Casquet, C., Galindo, C., Gonzalez-Casado, J.M., Alonso, A., Mas, R., Rodas, M., Garcia, E., Barrenechea, J.F. (1992): El metamorfismo de la Cuenca de los Cameros. Geocronología e implicaciones tectónicas. *Geogaceta*, 11: 22-25.

Cavazza, W. (1986): Miocene sediment dispersal in the central Española Basin, Rio Grande Rift, New Mexico, U.S.A. *Sedimentary Geology*, 51: 119-135.

Critelli, S., Le Pera, E. (1994): Detrital modes and provenance of Miocene sandstones and modern sands of the Southern Apennines thrust-top basins (Italy): *Journal of Sedimentary Research*, 64: 824–835.

Critelli, S., Le Pera, E., Ingersoll, R.V. (1997): The effects of source lithology, transport, deposition and sampling scale on the composition of southern California sand. *Sedimentology*, 44: 653–671.

Dickinson, W.R. (1985): Provenance relations from detrital modes of sandstones. In: G. G. Zuffa (ed.) *Provenance of arenites*. NATO ASI Series, C-148: 333-362

Dickinson, W.R., Suczek, C. A. (1979): Plate tectonics and sandstone compositions. *American Association of Petroleum Geologists Bulletin*, 63: 2164-2182.

Dickinson, W.R., Beard, L.S., Brakenridge, G.R., Erjavec, J.L., Ferguson, R.C., Inman, K.F., Knepp, R.A., Lindberg, F.A., Ryberg, P.T. (1983): Provenance of North American Phanerozoic sandstones in relation to tectonic setting. *Geological Society of America Bulletin*, 94: 222-235.

Evans, A.L. (1990): Miocene sandstone provenance relations in the Gulf of Suez: insights into synrift unroofing and uplift history. *American Association of Petroleum Geologists Bulletin*, 74: 1386-1400.

Fontana, D., Zuffa, G.G., Garzanti, E. (1989): The interaction of eustacy and tectonismfrom provenance studies of the Hecho Group Turbidite Complex (South-Central Pyrenees, Spain): *Basin Research*, 2: 223–237.

Garzanti, E., Vezzoli, G., Andò, S., Castiglione, G. (2001): Petrology of Rifted-margin sand (Red Sea and Gulf of Aden, Yemen). *Journal of Geology*, 109: 277-297.

Garzanti, E., Andò, S., Vezzoli, G., dell'Era, D. (2003): From rifted margins to Foreland Basins: Investigating provenance and sediment dispersal across Desert Arabia (Oman, U.A.E.). *Journal of Sedimentary Research*, 73: 572-588.

Gómez Fernández, J.C., Meléndez, N. (1994): Estratigrafía de la Cuenca de Cameros (Cordillera Ibérica Noroccidental, N de España) durante el tránsito Jurásico-Cretácico. *Revista de la Sociedad Geológica de España*, 7 (1–2): 121– 139.

González, L. Mas, R., Arribas, J. (2005): Provenance of fluvial sandstones at the beginning of the Latest Jurassic-Early Cretaceous Rift stage of the North Iberian Basin. *8th International Conference on Fluvial Sedimentology*. Delft, (Holland): Abstract book, 27p.

Graham, S.A., Ingersoll, R.V., Dickinson, W.R. (1976): Common provenance for lithic grains in Carboniferous sandstones from Ouachita Mountains and Black Warrior Basin. *Journal of Sedimentary Petrology*, 46 (3): 620-632.

Grantham, J.H., Velbel, M.A. (1988): The influence of climate and topography on rock-fragment abundance in modern fluvial sands of the southern Blue Ridge Mountains, North Carolina. *Journal of Sedimentary Petrology*, 58: 219-227.

Guimerà, J. (1984): Paleogene evolution of deformation in the northeastern Iberian Peninsula. *Geological Magazine*, 121: 413-420.

Guimerà, J., Alvaro, M. (1990): Structure et évolution de la compression alpine dans la Chaîne Ibérique et la Chaîne côtière catalane (Espagne). *Bulletin Société Géologique de France*, 6(2): 339-348.

Guimerà, J., Alonso, A., Mas, R. (1995): Inversion of an extensional-ramp basin by a newly formed thrust: the Cameros basin (N Spain). In: J.G. Buchanan and P.G. Buchanan (eds.): *Basin Inversion*. Geological Society Special Publication, 88: 433-453.

Guimerà J., Mas R., Alonso A. (2004): Intraplate deformation in the NW Iberian Chain: Mesozoic extension and Tertiary contractional inversion. *Journal of the Geological Society of London*, 161: 291-303.

Hubert, J.F., Feshbach-Meriney, P.E., Smith, M.A. (1992): The Triassic-Jurassic Hartford Rift Basin, Connecticut and Massachusetts: Evolution, sandstone diagenesis, and hydrocarbon history. *American Association of Petroleum Geologists Bulletin*, 76: 1710-1734.

Ibbeken, H., Schleyer, R. (1991): *Source and sediment. A case study of provenance and mass balance at an active plate margin (Calabria, Southern Italy)*. Springer-Verlag, Berlin, 286pp.

Ingersoll, R.V. (1978): Petrofacies and petrologic evolution of the Late Cretaceous fore-arc basin, northern and central California. *Journal of Geology*, 86: 335–352.

Ingersoll, R.V. (1983): Petrofacies and provenance of Late Mesozoic forearc basin, northern and central California. *American Association of Petroleum Geologists Bulletin*, 67: 1125-1142.

Ingersoll, R.V. (1990): Actualistic sandstone petrofacies: discriminating modern and ancient source rocks. *Geology*, 18: 733–736.

Ingersoll, R.V., Bullard, T.F., Ford, R.L., Grimm, J.P., Pickle, J.D., Sares, S.W. (1984): The effect of grain size on detrital modes: a test of the Gazzi-Dickinson point-counting method. *Journal of Sedimentary Petrology*, 54: 103-116.

Johnsson, M.J. (1993): The system controlling the composition of clastic sediments. In: M.J. Johnsson and A. Basu (eds.): *Processes Controlling the Composition of Clastic Sediments*. Geological Society of America. Special Paper, 284: 1-19.

Johnsson, M.J., Stallard, R.F., Lundberg, N. (1991): Controls on the composition of fluvial sands from a tropical weathering environment: Sands of the Orinoco River drainage basin, Venezuela and Colombia. *Journal of Geology*, 96: 263–277.

Leeder, M.R. (1995): Continental rifts and proto-oceanic rift troughs. In: C.J. Busby and R.V. Ingersoll (eds.): *Tectonics of Sedimentary Basins*. Oxford, U.K., Blackwell Science, p. 119–148.

Le Pera, E., Critelli, S. (1997): Sourceland controls on the composition of beach and fluvial sand of the northern Tyrrhenian coast of Calabria, Italy: implications for actualistic petrofacies. *Sedimentary Geology*, 110: 81–97.

Mack, G.H. (1981): Composition of modern stream sand in a humid climate derived from a low-grade metamorphic and sedimentary foreland fold-thrust belt of north Georgia. *Journal of Sedimentary Petrology*, 51: 1247-1258.

Mantilla-Figueroa, L.C., Casquet, C., Mas, J.R. (1998): Los paleofluidos del Grupo Oncala, Cuenca de Cameros (La Rioja, España): Datos de inclusiones fluidas, isótopos de Oxigeno y SEM. *Geogaceta*, 24: 207-210.

Mantilla-Figueroa, L. C., Casquet, C., Galindo, C., Mas, R. (2002-2005): El metamorfismo hidrotermal cretácico y paleógeno en la cuenca de Cameros (Cordillera Ibérica, España). *Zubía* 14: 143-154.

Martín-Closas, M., Alonso Millán, A. (1998): Estratigrafía y Bioestratigrafía (Charophyta) del Cretácico inferior en el sector occidental de la Cuenca de Cameros (Cordillera Ibérica). *Revista de la Sociedad Geológica de España*, 11: 253-269.

Mas, J.R., Alonso, A., Guimerá, J. (1993): Evolución tectonosedimentaria de una cuenca extensional intraplaca: La cuenca finijurásica-eocretácica de Los Cameros (La Rioja-Soria). *Revista de la Sociedad Geológica de España*, 6 (3-4): 129-144.

Mas, J.R., Guimera, J., Alonso, A. (1997): Evolution of a Mesozoic intraplate extensional basin: the Cameros Basin (North Spain). *Annual Meeting of IGCP Project Nº 369 Comparative Evolution of PeriTethyan Rift Basins*, 1: 33-36.

Mas, R., Benito, M. I., Arribas, J., Serrano, A., Guimerà, J., Alonso, A., Alonso-Azcárate, J. (2003): The Cameros Basin: From Late Jurassic-Early Cretaceous Extensión to Tertiary Contractional Inversion-Implications of Hydrocarbon Exploration. Northwest Iberian Chain, North Spain. *American Association of Petroleum Geologists, Geological Field Trip*, 11.

Mas, R., Benito, M.I., Arribas, J., Serrano, A.; Guimera, J., Alonso, A., Alonso-Azcarate, J. (2002-2005): La Cuenca de Cameros (Cordillera Ibérica Noroeste): desde la extensión finijurásica-eocretácica a la inversión contractiva terciaria - Implicaciones en la exploración de hidrocarburos. *Zubía,* 14: 9-64.

Najarro, M. (2005): Evolución sedimentaria, procedencia y diagénesis de los últimos episodios de relleno de la Cuenca de Cameros (Grupo Oliván, Cretácico Inferior, Cordillera Ibérica Septemtrional). Trabajo de Investigación. Fac. CC. Geológicas. UCM.

Najarro, M., Arribas, J., Mas, R., Ochoa, M. (2005): Sedimentary evolution and provenance of the last fluvial episodes of the Cameros Basin (Early Cretaceous, North Spain) *8th International Conference on Fluvial Sedimentology*. Delft, (Holland): Abstract book, 217p.

Nesbitt, H.W., Fedo, C.M., Young, G.M. (1997): Quartz and feldspar stability, steady and non-steady-state weathering, and petrogenesis of siliciclastic sands and muds: *Journal of Geology*, 105: 173–191.

Ochoa, M., Arribas, J., Mas, R. (2004): Changes in sandstone composition during Lower Cretaceous syn-rift fluvial sedimentation (Cameros Basin, Spain) *32nd International Geological Congress*. Florence (Italia): Abstract CD - Session 242-34.

Ochoa, M., Arribas, J., Mas, R., Najarro, M. (2005): Controls destroying a fluvial reservoir in Cameros Basin, Spain. 8th *International Conference on Fluvial Sedimentology*. Delft, (Holland): Abstract book, 226 p.

Palomares, M., Arribas, J. (1993): Modern stream sands from compound crystalline sources: composition and sand generation index. In: M.J. Johnsson and A. Basu (eds.): *Processes Controlling the Composition of Clastic Sediments*. Geological Society of America. Special Paper, 284: 313-322.

Pettijohn, F.J. (1957): *Sedimentary Rocks*, 2nd Edition, New York, Harper, 718 p.

Posamentier, H.W., Vail, P.R. (1988): Eustatic controls on clastic deposition, II, sequence and systems tract models. In: C.K. Wilgus *et al.* (ed.) *Sea level changes: An integrated approach*. Society of Economics, Paleontologists and Mineralogists, Special Publication, 42: 125-154.

Prosser, S. (1993): Rift-related linked depositional system and their seismic expression. In: G.D. Williams and A. Dobb (eds.): *Tectonics and Seismic Sequence Stratigraphy*. Geological Society of London, Special Publication, 71: 35–66.

Roca, E., Guimerà, J., Salas, R. (1994): Mesozoic extensional tectonics in the southeast Iberian Chain. *Geoogical Magazine*, 131 (2): 155-168.

Salas, R., Alonso, A., Aurell, M., Carbó, A., Casas. A., Gómez, J.C., Guimerà, J., Martín-Closas, C., Mas, R., Meléndez, A., Meléndez, G., Meléndez, N., Rivero, Ll., Serra-Kiel, J. (1992): Sequence stratigraphy and subsidence analysis of the Jurassic and Cretaceous in the Iberian basin (Iberian Range) Spain. *Sequence Stratigraphy of European Basins*. CNRS-IFP Dijon, France: Abstracts volume, 211.

Salas, R., Casas, A. (1993): Mesozoic extensional tectonics, stratigraphy and crustal evolution during the Alpine cycle of the eastern Iberian basin. *Tectonophysics*, 228: 33-55.

Salas, R., Guimerà, J., Mas, R., Martín-Closas, C., Meléndez, A., Alonso, A. (2001): Evolution of the Mesozoic Central Iberian Rift System and its Cenozoic inversion (Iberian Chain), In: P.A. Ziegler, W. Cavazza, A.H.F. Robertson and S. Crasquin-Soleau (eds.): *Peri-Thethyan Rift/Wrench Basins and Passive Margins*. Museum National D'Histoire Naturelle, Memoires, 186, Peri-Tethys Memoir 6: 145–186.

Soreghan, M.J., Cohen, A.S. (1993): The effects of basin asymmetry on sand composition: examples from lake Tanganyika, Africa. In: M.J. Johnsson and A. Basu (eds.): *Processes Controlling the Composition of Clastic Sediments*. Geological Society of America. Special Paper, 284: 285-301.

Valloni, R. (1985): Reading provenance from modern marine sands. In: G.G.Zuffa (Ed.) *Provenance of Arenites*. Dordrecht, D. Reidel: 309-332.

Vegas, R., Banda, E. (1982): Tectonic framework and Alpine evolution of the Iberian Peninsula. *Earth Evolution Sciences*, 4: 320-343.

Vera, J.A. (2001): Evolution of the South Iberian Continental Margin. In: P.A. Ziegler, W. Cavazza, A.H.F. Robertson and S. Crasquin-Soleau (eds.): *Peri-Thethyan Rift/Wrench Basins and Passive Margins*. Museum National D'Histoire Naturelle, Memoires, 186 Peri-Tethys, Memoir 6: 109-143

Vilas, L., Alonso, A., Arias, C., García, A., Mas, J.R., Rincón, R., Meléndez, N. (1983): The Cretaceous of the Southwestern Iberia Ranges (Spain). *Zitteliana*, 10: 245-254.

Weltje, G.J. (2002): Quantitative analysis of detrital modes: statistically rigorous confidence regions in ternary diagrams and their use in sedimentary petrology. *Earth-Science Reviews*, 57: 211-253.

Zuffa, G.G. (1980): Hybrid arenites: their composition and classification. *Journal of Sedimentary Petrology*, 50: 21-29.

Zuffa, G.G. (1991): On the use of turbidite arenites in provenance studies: critical remarks. *Geological Society, Special. Publication*, 57: 23-30.

Zuffa, G.G., Gaudio, W., Rovito, S. (1980): Detrital mode evolution of the rifted continental-margin Longobucco sequence (Jurassic), Calabrian Arc, Italy. *Journal of Sedimentary Petrology*, 50: 51-61.

Zuffa, G.G., Cibin, U., Di Giulio, A. (1995): Arenite petrography in sequence stratigraphy. *Journal of Geology*, 103: 451–459.